


Article

# The Initial-Final Mass Relation from Carbon Stars in Open Clusters

Carlos Abia <sup>1,\*</sup>, Inma Domínguez <sup>1</sup>, Paola Marigo <sup>2</sup>, Sergio Cristallo <sup>3,4</sup> and Oscar Straniero <sup>3</sup><sup>1</sup> Department Física Teórica y del Cosmos, Universidad de Granada, E-18071 Granada, Spain; inma@ugr.es<sup>2</sup> Department of Physics and Astronomy G. Galilei, University of Padova, Vicolo dell'Osservatorio 3, I-35122 Padova, Italy; paola.marigo@unipd.it<sup>3</sup> INAF—Osservatorio Astronomico d'Abruzzo, Via Maggini snc, I-64100 Teramo, Italy; sergio.cristallo@inaf.it (S.C.); oscar.straniero@inaf.it (O.S.)<sup>4</sup> INFN—Sezione di Perugia, Via A. Pascoli snc, I-06126 Perugia, Italy

\* Correspondence: cabia@ugr.es; Tel.: +34-958249061

**Abstract:** Recently, Marigo et al, identified a kink in the initial-final mass relation around initial masses of  $M_{ini} \approx 1.65 - 2.10 M_{\odot}$ , based on Gaia DR2 and EDR3 data for white dwarfs in open clusters aged 1.5–2.5 Gyr. Notably, the white dwarfs associated with this kink, all from NGC 7789, exhibit masses of  $\sim 0.70-0.74 M_{\odot}$ , usually associated with stars of  $M_{ini} \sim 3-4 M_{\odot}$ . This kink in the  $M_{ini}$  mass range coincides with the theoretically accepted solar metallicity lowest-mass stars evolving into carbon stars during the AGB phase. According to Marigo et al., these carbon stars likely experienced shallow third dredge-up events, resulting in low photospheric C/O ratios and, consequently, middle stellar winds. Under such conditions, the AGB phase is prolonged, allowing for further core mass growth beyond typical predictions. If this occurs, it might provoke other anomalies, such as a non-standard surface chemical composition. We have conducted a chemical analysis of several carbon stars belonging to open clusters within the above cluster ages. Our chemical analysis reveals that the carbon stars found within the kink exhibit C/O ratios only slightly above the unity and the typical chemical composition expected for carbon stars of near solar metallicity, partially validating the above theoretical predictions. We also show that this kink in the IMFR strongly depends on the method used to derived the distances (luminosity) of these carbon stars.

**Keywords:** carbon stars; nucleosynthesis; stellar evolution; white dwarfs

**Citation:** Abia, C.; Domínguez, I.; Marigo, P.; Cristallo, S.; Straniero, O. The Initial-Final Mass Relation from Carbon Stars in Open Clusters. *Galaxies* **2024**, *12*, 67. <https://doi.org/10.3390/galaxies12060067>

Academic Editor: Oleg Malkov

Received: 14 September 2024

Revised: 10 October 2024

Accepted: 21 October 2024

Published: 23 October 2024



**Copyright:** © 2024 by the authors. Licensee MDPI, Basel, Switzerland. This article is an open access article distributed under the terms and conditions of the Creative Commons Attribution (CC BY) license (<https://creativecommons.org/licenses/by/4.0/>).

## 1. Introduction

The final stages of the evolution of low- and intermediate-mass stars ( $1 \lesssim M/M_{\odot} \lesssim 8$ ), particularly during the asymptotic giant branch (AGB) phase, remain poorly understood. This phase is challenging to model due to the complexity of physical processes such as the third dredge-up (3DU), hot-bottom burning (HBB), and their dependence on the initial stellar mass, metallicity, and mass loss. These phenomena are very sensitive to the treatment of convection and mixing, to the numerical details and prescription for the mass loss used (e.g., [1–5]).

In this context, observations play a key role, as they can place constraints on the processes mentioned above whose physics are still poorly defined. In the solar-like metallicity regime, a relevant source of information comes from the semi-empirical initial–final mass relation (IFMR), which links the initial mass of low- and intermediate-mass stars with the final mass of white dwarfs left behind on their death (e.g., [6–9]). The IFMR is very sensitive to the prescriptions used to model the mass loss, 3DU, and hot-bottom burning of the progenitor stars (e.g., [10,11]). Thus, observational studies of the IFMR can put constrains on all these phenomena. However, these studies in the Milky Way have so far been hampered by severe uncertainties on the distances of the stars, and by the fact that the AGB population in star clusters (whose distances are better known than those of field AGB

stars) is very small. This situation has now remarkably improved thanks to the advent of the Gaia satellite and its data releases, in particular Gaia DR3 [12]. In fact, with the addition of new white dwarf data belonging to galactic open clusters with ages of 1.5–2.5 Gyr, [11,13] found a kink in the IFMR at  $M_{ini} \approx 1.65\text{--}2.10 M_{\odot}$  that suddenly interrupts the commonly assumed monotonic behaviour. Surprisingly, the white dwarfs at the peak, which are all members of the open cluster NGC 7789, may reach masses of  $0.70\text{--}0.74 M_{\odot}$  according to these authors, which have previously been associated with stars with  $M_{ini} \sim 3\text{--}4 M_{\odot}$ . The IFMR kink is interpreted by these authors as a signature of the lowest mass stars in the Milky Way that evolved into carbon stars (C-stars) during the AGB phase. According to [13], these C-stars are expected to have undergone shallow 3DU events, resulting in a low photospheric C/O ratio (very close to unity). This is because the mass-loss prescription for carbon stars used by [13] is dependent on carbon excess ([14–16]), and under this condition carbonaceous dust grains cannot condense in sufficient quantities to cause a strong wind, so the AGB lifetime is prolonged and the core mass can grow more than usually predicted.

Apart of a low C/O ratio and mass-loss rate, we wondered if the carbon stars with masses within the possible kink in the IFMR could have also other observational signatures that may characterise them, in particular a different chemical composition with respect to that usually observed in most of the galactic field carbon stars. Thus, we performed a full chemical analysis of several galactic carbon stars belonging to galactic open cluster of near solar metallicity with ages within those where the kink in the IFMR could exist, by using high resolution and signal-to-noise spectra. In the next section we describe the observations and the spectroscopic analysis. Section 3 shows the main results of the chemical analysis and in Section 4 we derive the luminosity of these stars using Gaia DR3 data and construct our own IMFR under different approximations. Section 5 summarises our main findings.

## 2. Observations and Analysis

The observations were made in June and August 2023 at the 3.5 m telescope in the CAHA observatory using the CARMENES spectrograph, and at the Observatory of the Roque de los Muchachos with the 3.6 m TNG facility using the GIANO-B and HARPS-N spectrographs working together in the GIARPS mode. The CARMENES spectrograph provides high spectral resolution ( $R = 80,000\text{--}100,000$ ) in the  $0.52\text{--}0.96 \mu\text{m}$  and  $0.96\text{--}1.71 \mu\text{m}$  spectral ranges, while the TNG observing in GIARPS mode covers the  $0.97\text{--}2.45 \mu\text{m}$  ( $R = 50,000$ ) and  $0.38\text{--}0.69 \mu\text{m}$  ( $R = 115,000$ ) spectral ranges. These two instrumental set-ups allowed us to access to most of the spectral ranges suited for abundance analysis of cool C-stars, namely: the carbon and oxygen abundances and the corresponding C/O and  $^{16}\text{O}/^{17}\text{O}$  ratios from the  $2.2 \mu\text{m}$  region; the  $^{12}\text{C}/^{13}\text{C}$  ratio from the  $\sim 8000 \text{ \AA}$  region; s-element (Zr, Ba and Ce mainly) abundances from the  $\sim 4800 \text{ \AA}$ ,  $\sim 8100 \text{ \AA}$  and  $1.5\text{--}1.7 \mu\text{m}$  spectral regions; the fluorine abundance from several HF lines at  $\sim 2.3 \mu\text{m}$ , and finally the Li abundance from the typical  $6708 \text{ \AA}$  line. The average metallicity of the star ( $[M/H]$ )<sup>1</sup> was derived from several Fe, Ti, Ni and Ca placed in these spectral ranges. For details about the specific molecular and atomic lines used, as well as a full discussion on the uncertainty in the chemical features derived in the abundance analysis we refer to [17–21], and references therein. The S/N ratio of the spectra achieved typically ranged from  $>50$  in the  $4800 \text{ \AA}$  region to  $S/N > 300$  at near infrared wavelengths. Our previous abundance studies in C-stars (see references above) showed that these values are high enough to perform an accurate abundance analysis in all the spectral ranges studied.

Table 1 shows the C-stars observed together with the name of the open cluster they belong to, age of the cluster derived by [22] based on Gaia EDR3 astrometry, and the probability of membership to the corresponding open cluster according to the analysis of [13]. All the stars were included in the study by [13], and have excellent Gaia DR3 astrometric solutions: uncertainty in the parallax  $< 10\%$ , fidelity flag  $\sim 1$ , RUWE values  $< 1.4$  (i.e., no-binary) and available 2MASS photometry with JHK magnitude uncertainties  $< 10\%$ .

**Table 1.** C-stars observed, open cluster name, age of the cluster and probability membership.

Name	Open Cluster	Log (Age)	<i>p</i>
V493 Mon	Trumpler 5	9.63	0.68
C* 908	Ruprecht 37	9.37	0.99
MSB 75	NGC 7789	9.20	0.99
Case 63	Berkeley 9	9.14	0.99
Case 473	Berkeley 53	8.99	0.68
IRAS 19582+2907	FSR 0172	8.20	0.99
Case 121	Berkeley 72	7.73	0.99
Case 588	Dias 2	9.24	0.99
DH Mon	Ruprecht 37	9.37	0.68

\* Ages are taken from Cavallo et al. (2024), [22].

Note that the stars IRAS 19582+2907 and Case 121 belong to open clusters with ages (according to [22]) corresponding to turn-off masses larger than  $\sim 4 M_{\odot}$ . Thus, theoretically, these stars would not be C-stars but O-rich AGBs and probable candidates to HBB stars. However, their spectra indeed look like a normal C-star, and we will show below that their chemical composition is similar to the other C-stars analysed. The conclusion is then that whether these stars do not belong to the quoted open cluster or the age of Berkeley 72 and FSR 0172 was largely underestimated by [22]. In particular, the carbon star MSB 75 belongs to the cluster NGC 7789 where three white dwarfs exhibit masses in excess of  $\sim 0.7 M_{\odot}$  according to [8]. Furthermore, according to [13] the stars Case 63 and Case 588 have  $M_{ini}$  inside the mass range where the kink is proposed to exist. The rest of the stars belong to clusters with ages close to that of NGC 7789, where the kink in the IFMR was identified.

For each star we computed synthetic LTE spectra in the mentioned spectral ranges using the Turbospectrum v.20 code ([23]) and atmosphere models for C-stars (unpublished) built following the approximations and method in [24]. Because the young ages of the clusters, initially we assumed a solar metallicity for all the stars. The final metallicity was obtained as the average of the metallicity derived from theoretical fits to the metallic lines mentioned above. This resulted in a good approximation (see below), except in the case of Case 588 (Dias 2) for which, we derived  $[M/H] \sim -1$ . As an initial estimate of the effective temperature, the values derived by [13] using SED fits were adopted, the final value however was determined from an iterative method changing the  $T_{eff}$  value until a reasonable fit to the observed spectrum was obtained in all the spectral ranges studied. We adopted a  $\log g$  value of 0.0 for all the stars because we do not have other gravity value in the grid of C-stars models. However, this is an acceptable value for stars in the AGB phase. Next step was to derive the C/O ratio by iterative fits to some CO lines in the  $2.3 \mu\text{m}$  region, and CN lines in the  $\sim 8000\text{--}8600 \text{ \AA}$  spectral region, respectively, until convergence was achieved. Finally, with values of the effective temperature, gravity, average metallicity and C/O ratio, we proceeded with the full chemical analysis of the stars. To do that we computed theoretical spectra in LTE with the Turbospectrum code using the adequate model atmosphere for the spectral ranges analysed (see above) and changed the abundance of a given chemical specie until a good fit was found between the observed (atomic or molecular) and theoretical spectral line. Typical examples of these theoretical fits for similar carbon stars belonging to the galactic field can be seen in references [17–20].

### 3. Results

Table 2 shows the main chemical features derived in the stars. From left to right the columns show: name of the star, the average metallicity, the carbon to oxygen ratio (by number), the carbon isotopic ratio, the nitrogen isotopic ratio, the oxygen-16 to oxygen-17 isotopic ratio, the Li abundance in the usual scale of  $\log N(\text{H}) \equiv 12$ , the fluorine abundance ratio and the average s-element abundance ratio derived from some Zr, Ba, Ce lines, respectively. We note that most of the stars have near solar metallicity, except Case 588, which is clearly a metal-poor star as mentioned above. Furthermore, the C/O ratios are

all only slightly larger than unity; the larger value is found also for Case 588 (1.41), which agrees with the theoretical expectation that the 3DU is more efficient in metal-poor stars, so larger C/O ratios are expected in the surface of these C-stars. The low C/O ratios found almost in all the stars studied agrees with the theoretical expectation by [13,25] in case that shallow 3DUs occur in the particular  $M_{ini}$  range where the kink in the IFMR is observed. However this characteristic is found in the overwhelming majority of the galactic field AGB C-stars so far analysed (see [17]). In fact other plausible explanations have been proposed to explain this observational fact. For instance, [26] suggested that as the carbon is transported to the surface by the action of the 3DU episodes and the star progressively cools-down in its ascent into the AGB phase, the carbon atoms would condense into amorphous graphite, TiC and SiC grains in the cool surface of the star. Then the gas phase in the surface is continuously depleted in carbon because the condensation into grains. This may provoke that in the gas phase (what we actually see in the visual and near-infrared spectrum) the C/O ratio will never exceed unity significantly. This process, however, is highly dependent on the metallicity of the star: in metal-poor carbon stars C/O ratios exceeding largely unity can be found as is the case of our only metal-poor star in the sample, Case 588 (see Table 2).

**Table 2.** Abundance ratios derived in the stars.

Star	[M/H]	C/O	$^{12}\text{C}/^{13}\text{C}$	$^{14}\text{N}/^{15}\text{N}$	$^{16}\text{O}/^{17}\text{O}$	A(Li)	[F/M]	[<s>/M]
V493 Mon	−0.4	<1.5	<25	-	-	-	-	-
C* 908	−0.3	1.07	50	1000	-	0.0	-	0.25
MSB 75	−0.25	1.05	35	>700	650	−0.6	−0.1	0.4
Case 63	−0.1	1.05	52	1250	580	−2.0	0.15	0.32
Case 473	0.0	1.07	58	-	670	−1.0	0.3	<0.5
IRAS19582+2907	0.0	1.04	50	-	-	−0.5	-	0.6
Case 121	−0.2	1.07	55	>1000	1000	−1.0	−0.1	0.2
Case 588	−1.0	1.41	70	800	-	−0.6	-	1.0
DH Mon	−0.3	1.06	10	200–500	-	+0.6	-	No

Considering the typical uncertainties in the features of Table 2:  $\pm 0.25$  dex for the [M/H], [F/M] ratios;  $\pm 0.3$  dex for [<s>/M];  $\pm 0.03$  for C/O;  $\pm 10$  for  $^{12}\text{C}/^{13}\text{C}$ ; a factor of two for  $^{14}\text{N}/^{15}\text{N}$ ;  $\pm 300$  for  $^{16}\text{O}/^{17}\text{O}$  and  $\pm 0.2$  dex for Li abundance (a full discussion of the derivation of these uncertainties can be found in references [17–21]), the carbon, nitrogen and oxygen isotopic ratios derived are also quite similar to those found in normal field C-stars (see references above) (by passing, indicating no evidence of the operation of the HBB). On the other hand, Li is heavily depleted as expected (see, e.g., [27]) except in DH Mon (see below), and the fluorine and s-element ratios respect to the average metallicity are also those typically found in normal C-stars: i.e., low or middle enhancements. Thus, globally the chemical abundances and abundance ratios derived in these C-stars are similar to those found in field galactic C-stars. Only the star DH Mon shows a chemical pattern rather different. This star has low  $^{12}\text{C}/^{13}\text{C}$  and  $^{15}\text{N}/^{14}\text{N}$  ratios, some Li enhancement and no s-element enhancements at all. These are typically the chemical features defining the J-type AGB stars; we conclude that DH Mon probably is an AGB star of this type. This is quite interesting because considering the age of its host cluster ( $\sim 2.3$  Gyr, Ruprecht 37), this may put constraints to the scenarios proposed for the formation of these kind of carbon stars whose origin is still unknown (e.g., [28,29]). Note also that the fact of a low  $^{14}\text{N}/^{15}\text{N}$  ratio in this star reinforces the idea suggested by [19] that J-type stars might be a source of the AB-type grains ([30]). On the other hand, among the carbon stars that [13] place just in the kink of the IFMR (Case 63, Case 588 and MSB 75), we do not find significant differences in their chemical features considering the typical uncertainties mentioned above. Only, as already mentioned, Case 588 shows a larger C/O value and [<s>/M] ratio than the others two objects due to its considerably lower metallicity, which agrees with theoretical expectations (see, e.g., [25]). In brief, all the stars analysed show similar chemical properties

among them (except the possible J-type star DH Mon), and similar to those so far derived in carbon stars of the galactic field with similar metallicities.

#### 4. Luminosity and the IFMR

In previous sections we have shown that the C-stars analysed do not present any chemical anomaly compared with other C-stars. Now, we compare the chemical patterns found for individual stars with theoretical nucleosynthesis predictions during the AGB phase. To do that, we have first to estimate the luminosity of the stars; then we will build our own IFMR. For this we adopt two approximations:

- Case 1: We adopted the individual Gaia DR3 geometrical distances according to [31] without any zero-point correction. The extinction for each star  $A_v$  is derived from the galactic model by [32] and bolometric corrections in the K-band were taken from [33].
- Case 2: We adopted the distances and extinctions of the open cluster to which each star belongs to according to [22], and the same bolometric corrections as in Case 1.

The total uncertainty in the luminosity derived in both Cases is  $\pm 0.25$  mag (see [34]). The luminosity obtained in these two approximations must be compared with those derived by [13] using Gaia EDR3 purely parallax-based distances; extinctions from [35] or [36] based on Gaia DR2 astrometry, and theoretical fits to individual SEDs.

We found that Cases 1 and 2 result in very similar luminosity values, although in Case 2 the average bolometric and K magnitudes show a smaller dispersion: mean values  $M_K = -8.17 \pm 0.30$  mag, and  $M_{bol} = -5.06 \pm 0.30$  mag. These magnitude values agree very well with the average absolute K-magnitude found in C-stars of the Magellanic Cloud ([37]) and with the average bolometric magnitude found recently in galactic field C-stars by [34]. Thus, in the following we adopted the luminosities obtained in Case 2. We have to emphasise that the differences in the luminosity between the different methods are due mainly to differences in the distance; extinction only plays a minor role. In general, the method used by [13] result in larger distances thus, higher luminosities, which implies larger core masses. For instance, the mean difference in the distances between [13] and Case 2 is  $120 \pm 633$  pc. Note the large dispersion, which means that for some stars the discrepancy in the distance is severe (mainly for stars at distances  $> 3$  kpc).

Then, assuming the luminosities derived in Case 2, we compare with theoretical nucleosynthesis predictions for AGB stars from the FRUITY database ([38]), just at the luminosity and metallicity (within the observational uncertainties, see Table 2) derived for each star. In general, we found that FRUITY predictions for the 1.5–2.0  $M_\odot$  AGB models can account for all the chemical features (within the uncertainties) found in the stars. This excludes the probable J-type star DH Mon and the Mira variable V493 Mon, which shows very broad spectral lines probably due to stellar pulsations. However, FRUITY fails to fit the C/O ratios derived, which are predicted to be larger than observed. Nevertheless, this is a long-standing problem (see discussion, e.g., in [3]). The 2.5  $M_\odot$  models can account partially for the observed abundance patterns, while the 3.0  $M_\odot$  models can not fit any of the chemical features derived. Thus, our objects should have masses not much larger than  $\sim 2 M_\odot$ , which agrees with the common idea that C-stars are low mass objects.

Then, we constructed our IFMR with the stars analysed. To do that we estimate the core mass (i.e.,  $M_{final}$ ), according to the FRUITY database, as just that which the star has during the AGB phase in which it best adjusts its derived luminosity in Case 2. Note that this core mass would be only slightly smaller than the final core mass after the star ends the AGB phase. In our case they range typically between 0.55 and 0.64  $M_\odot$  (see Figure 1). On the other hand, the  $M_{ini}$  value was estimated from the corresponding turn-off mass of the open cluster adopting the ages from [22]. Obviously, this mass would be only slightly smaller than the real mass of the star. Note that the age that best fit the position of the stars in the HR-diagram (according to the FRUITY database) are fully compatible (within the uncertainties) with the age of the cluster from [22]. The result of all of this (blue points) can be seen in the IMFR of Figure 1, where it is superimposed with the IMFR derived by [8] (grey points, note that these points are white dwarfs, not carbon stars)<sup>2</sup>. Because the ages



of the clusters in Table 1 is still rather controversial, we have added a blue horizontal line in Figure 1 to each star to indicate the possible range in  $M_{ini}$  of the corresponding star according to the different ages (turn-off masses) existing in the literature for the specific open cluster the star belongs to ([22,35,36,39]), all based on Gaia DR2 or DR3 data). It is clear that from Figure 1 that no kink in the IFMR is seen around  $M \sim 1.65\text{--}2.10 M_{\odot}$ . Our analysis is compatible with a linear behaviour in this mass range.

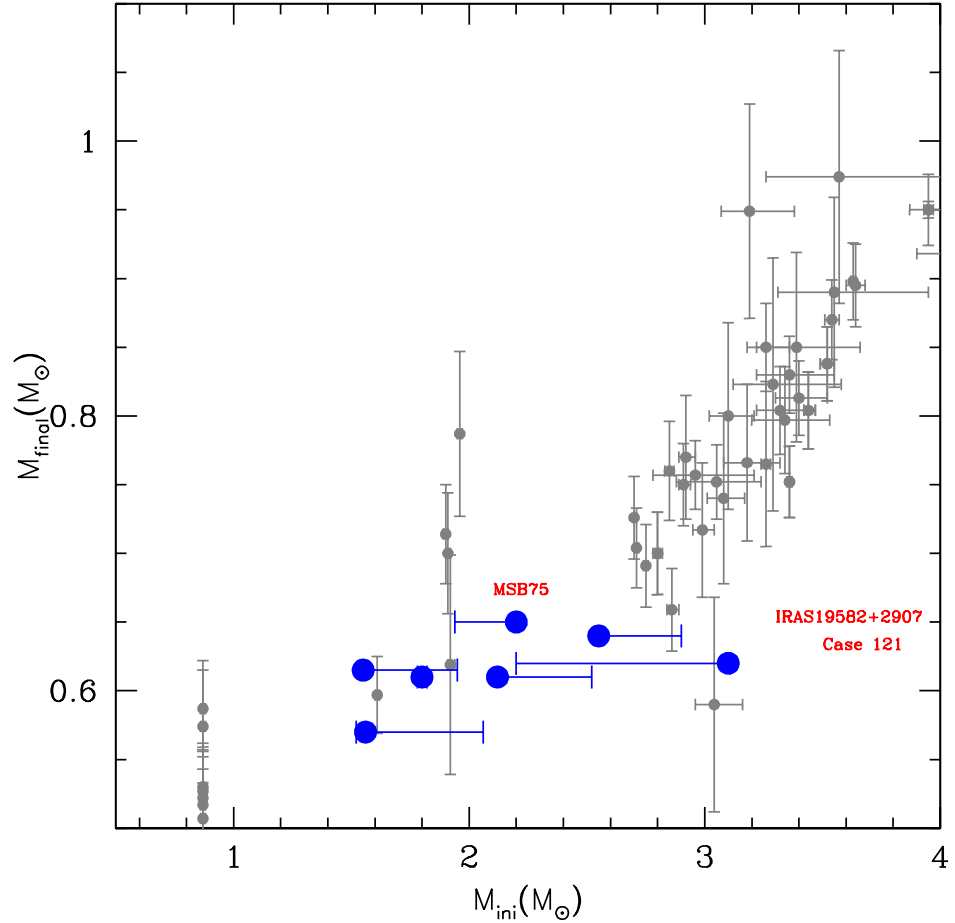


**Figure 1.** The IFMR derived in this work (blue dots) for the stars studied (see text). Grey dots show the IFMR by [8] derived on the basis of white dwarfs analysis. It is marked (red) the location of the star MSB 75, which belongs to the cluster NGC 7789 where some white dwarfs exceeding  $0.7 M_{\odot}$  have been found and suggest the existence of the kink ([11,13]). The virtual location of the C-stars IRAS 19582+2907 and Case 121 are also indicated (red); both stars apparently should have an initial mass  $M_{ini} > 4 M_{\odot}$  (see text).

## 5. Summary

We performed a detailed chemical analysis of several AGB C-stars belonging to Galactic open clusters with ages corresponding to initial masses of around  $1.65\text{--}2.15 M_{\odot}$ . These stars are located within the possible kink (discontinuity) in the semi-empirical IFMR suggested by [11,13]. Our analysis shows that these stars exhibit chemical features identical to other field AGB C-stars of comparable metallicities. Interestingly enough, most of these stars display C/O ratios slightly above unity, aligning with theoretical predictions ([13,25]) for stars that might populate this kink. However, this characteristic has been found in the overwhelming majority of Galactic C-stars analysed so far. We showed that the luminosities—and consequently the core mass ( $M_{final}$ )—of these stars are highly sensitive to the method used for determining their distance, despite all methods being based on Gaia DR3 astrometry. We find that purely parallax-based distances, as adopted in [13],

tend to result in larger distances (luminosity) than those derived from the methods used in this study, particularly for stars beyond  $\sim 3000$  pc. Indeed, some of the stars placed within the supposed kink in the IFMR have distances larger than the above value. Thus, the luminosity derived and, therefore, their estimated  $M_{ini}$  and  $M_{final}$  would be significantly larger if purely parallax distances are used compared to other methods. Extinction only plays a minor role in this. Clearly, more accurate distance measurements and stellar statistics in open clusters (in both white dwarfs and AGB stars) are needed to resolve the question of whether the discontinuity in the IMFR truly exists.

**Author Contributions:** All the authors in this research have equally participated in the elaboration of the paper. All authors have read and agreed to the published version of the manuscript.

**Funding:** This research has been partially funded by the project PID2021-123110NB-I00 financed by MICIU/AEI/10.13039/501100011033 and by FEDER, Una manera de hacer Europa, UE.

**Data Availability Statement:** The datasets presented in this article are not readily available because the data are part of an ongoing study. Requests to access the datasets should be directed to Carlos Abia.

**Conflicts of Interest:** The authors declare no conflicts of interest

### Abbreviations

The following abbreviations are used in this manuscript:

AGB	Asymptotic giant branch
2MASS	Two micron sky survey
IFMR	Initial final mass relation
SED	Spectrum energy distribution
FRUITY	FRANEC repository of updated isotopic tables & yields

### Notes

- <sup>1</sup> We adopt here the usual notation  $[X/H] = \log(X/H)_* - \log(X/H)_\odot$ , where  $(X/H)_*$  is the abundance by number of the element X in the corresponding star.
- <sup>2</sup> We remark again that the discussion by [11,13] on the possibility of the existence of a kink in the IFMR, is mainly based on the three white dwarfs in Figure 1 located around  $M_{ini} \sim 1.9 M_\odot$  with a  $M_{final} \geq 0.7 M_\odot$ , all belonging to NGC 7789 (see [8]).

### References

1. Frost, C.A.; Lattanzio, J. On the numerical treatment and dependence of the third dredge-up phenomenon. *Astrophys. J.* **1996**, *473*, 383–387. [[CrossRef](#)]
2. Ventura, P.; D’Antona, F. Full computation of massive AGB evolution. I. The large impact of convection on nucleosynthesis. *Astron. Astrophys.* **2005**, *438*, 279–288. [[CrossRef](#)]
3. Straniero, O.; Abia, C.; Domínguez, I. The carbon star mystery: 40 years later. *Eur. Phys. J. A* **2023**, *59*, 17. [[CrossRef](#)]
4. Cristallo, S.; Straniero, O.; Gallino, R.; Piersanti, L.; Domínguez, I.; Lederer, M.T. Evolution, nucleosynthesis, and yields of low-mass asymptotic giant branch stars at different metallicities. *Astrophys. J.* **2009**, *696*, 797–820. [[CrossRef](#)]
5. Marigo, P.; Bressan, A.; Nanni, A.; Girardi, L.; Pumo, M.L. Evolution of thermally pulsing asymptotic giant branch stars—I. The COLIBRI code. *Mon. Not. R. Astron. Soc.* **2013**, *434*, 488–526. [[CrossRef](#)]
6. Catalan, S.; Isern, J.; García-Berro, E.; Ribas, I. The initial-final mass relationship of white dwarfs revisited: Effect on the luminosity function and mass distribution. *Mon. Not. R. Astron. Soc.* **2008**, *387*, 1693–1703. [[CrossRef](#)]
7. Salaris, M.; Serenelli, A.; Weiss, A.; Bertolami, M.M. Semi-empirical White Dwarf Initial-Final Mass Relationships: A Thorough Analysis of Systematic Uncertainties Due to Stellar Evolution Models. *Astrophys. J.* **2009**, *692*, 1013–1032. [[CrossRef](#)]
8. Cummings, J.D.; Kalirai, J.S.; Tremblay, P.E.; Ramirez-Ruiz, E.; Choi, J. The White Dwarf Initial-Final Mass Relation for Progenitor Stars from 0.85 to 7.5  $M_\odot$ . *Astrophys. J.* **2018**, *866*, 21. [[CrossRef](#)]
9. Cunningham, T.; Tremblay, P.-E.; O’Brien, M.W. Initial-final mass relation from white dwarfs within 40 pc. *Mon. Not. R. Astron. Soc.* **2024**, *527*, 3602–3611. [[CrossRef](#)]
10. Kalirai, J.S.; Marigo, P.; Tremblay, P.-E. The Core Mass Growth and Stellar Lifetime of Thermally Pulsing Asymptotic Giant Branch Stars. *Astrophys. J.* **2014**, *782*, 17. [[CrossRef](#)]

11. Marigo, P.; Cummings, J.D.; Curtis, J.L.; Kalirai, J.; Chen, Y.; Tremblay, P.-E.; Ramirez-Ruiz, E.; Bergeron, P.; Bladh, S.; Bressan, A.; et al. Carbon star formation as seen through the non-monotonic initial-final mass relation. *Nat. Astron.* **2020**, *4*, 1102–1110. [[CrossRef](#)]
12. Brown, A.G.A.; Vallenari, A.; Prusti, T.; De Bruijne, J.; Babusiaux, C.; Biermann, M.; Creevey, O.; Evans, D.; Eyer, L.; Hutton, A.; et al. Gaia Early Data Release 3. Summary of the contents and survey properties. *Astron. Astrophys.* **2021**, *649*, A1.
13. Marigo, P.; Bossini, D.; Trabucchi, M.; Addari, F.; Girardi, L.; Cummings, J.D.; Pastorelli, G.; Tio, P.D.; Costa, G.; Bressan, A. A fresh look at AGB stars in galactic open cluster with Gaia: Impact on stellar models and the initial-final mass relation. *Astrophys. J. Suppl. Ser.* **2022**, *258*, 1–37. [[CrossRef](#)]
14. Mattsson, L.; Wahlin, R.; Höfner, S. Dust driven mass loss from carbon stars as a function of stellar parameters. I. A grid of solar-metallicity wind models. *Astron. Astrophys.* **2010**, *509*, A14. [[CrossRef](#)]
15. Eriksson, K.; Nowotny, W.; Höfner, S.; Aringer, B.; Wachter, A. Synthetic photometry for carbon-rich giants. IV. An extensive grid of dynamic atmosphere and wind models. *Astron. Astrophys.* **2014**, *566*, A14. [[CrossRef](#)]
16. Bladh, S.; Eriksson, K.; Marigo, P.; Liljegren, S.; Aringer, B. Carbon star wind models at solar and sub-solar metallicities: A comparative study. I. Mass loss and the properties of dust-driven winds. *Astron. Astrophys.* **2019**, *623*, A119. [[CrossRef](#)]
17. Abia, C.; Domínguez, I.; Gallino, R.; Busso, M.; Maserà, S.; Straniero, O.; de Laverny, P.; Plez, B.; Isern, J. s-Process Nucleosynthesis in Carbon Stars. *Astrophys. J.* **2002**, *579*, 817–837. [[CrossRef](#)]
18. Abia, C.; Cunha, K.; Cristallo, S.; Laverny, P.D. The origin of fluorine: Abundances in AGB carbon stars revisited. *Astron. Astrophys.* **2015**, *581*, A88. [[CrossRef](#)]
19. Hedrosa, R.P.; Abia, C.; Busso, M.; Cristallo, S.; Domínguez, I.; Palmerini, S.; Plez, B.; Straniero, O. Nitrogen Isotopes in Asymptotic Giant Branch Carbon Stars and Presolar SiC Grains: A Challenge for Stellar Nucleosynthesis. *Astrophys. J.* **2013**, *768*, L11. [[CrossRef](#)]
20. Abia, C.; Hedrosa, R.P.; Domínguez, I.; Straniero, O. The puzzle of the CNO isotope ratios in asymptotic giant branch carbon stars. *Astron. Astrophys.* **2017**, *599*, A39. [[CrossRef](#)]
21. Cunha, K.; Smith, V.V.; Hasselquist, S.; Souto, D.; Shetrone, M.D.; Prieto, C.A.; Bizyaev, D.; Frinchaboy, P.; García-Hernández, D.A.; Holtzman, J.; et al. Adding the s-Process Element Cerium to the APOGEE Survey: Identification and Characterization of Ce II Lines in the H-band Spectral Window. *Astrophys. J.* **2017**, *844*, 145. [[CrossRef](#)]
22. Cavallo, L.; Spina, L.; Carraro, G.; Magrini, L.; Poggio, E.; Cantat-Gaudin, T.; Pasquato, M.; Lucatello, S.; Ortolani, S.; Schiappacasse-Ulloa, J. Parameter Estimation for Open Clusters using an Artificial Neural Network with a QuadTree-based Feature Extractor. *Astron. J.* **2024**, *167*, 1. [[CrossRef](#)]
23. Plez, B. *Turbospectrum: Code for Spectral Synthesis*; Astrophysics Source Code Library. 2012
24. Gustafsson, B.; Edvardsson, B.; Eriksson, K.; Jørgensen, U.G.; Nordlund, Å.; Plez, B. A grid of MARCS model atmospheres for late-type stars. I. Methods and general properties. *Astron. Astrophys.* **2008**, *486*, 951–970. [[CrossRef](#)]
25. Addari, F.; Marigo, P.; Bressan, A.; Costa, G.; Shepherd, K.; Volpato, G. The Role of the Third Dredge-up and Mass Loss in Shaping the Initial-Final Mass Relation of White Dwarfs. *Astrophys. J.* **2024**, *964*, 51. [[CrossRef](#)]
26. Lodders, K.; Fegley, B. Condensation chemistry of carbon stars. *AIP Conf. Proc.* **1997**, *402*, 391–423.
27. Palmerini, S.; Cristallo, S.; Busso, M.; Abia, C.; Uttenthaler, S.; Gialanella, L.; Maiorca, E. Deep Mixing in Evolved Stars. II. Interpreting Li Abundances in Red Giant Branch and Asymptotic Giant Branch Stars. *Astrophys. J.* **2011**, *741*, 1. [[CrossRef](#)]
28. Zhang, X.; Jeffery, C.S. White dwarf-red giant mergers, early-type R stars, J stars and lithium. *Mon. Not. R. Astron. Soc.* **2013**, *430*, 2113–2120. [[CrossRef](#)]
29. Sengupta, S.; Izzard, R.G.; Lau, H.H.B. A nova re-accretion model for J-type carbon stars. *Astron. Astrophys.* **2013**, *599*, A66. [[CrossRef](#)]
30. Davis, A.M. Cosmochemistry special feature: Stardust in meteorites. *Proc. Natl. Acad. Sci. USA* **2011**, *108*, 19142–19146. [[CrossRef](#)]
31. Bailer-Jones, C.A.L.; Rybizki, J.; Fouesneau, M.; Demleitner, M.; Andrae, R. Estimating Distances from Parallaxes. V. Geometric and Photogeometric Distances to 1.47 Billion Stars in Gaia Early Data Release 3. *Astron. J.* **2021**, *161*, 147. [[CrossRef](#)]
32. Lallement, R.; Vergely, J.L.; Babusiaux, C.; Cox, N.L.J. Updated Gaia-2MASS 3D maps of Galactic interstellar dust. *Astron. Astrophys.* **2022**, *661*, A147. [[CrossRef](#)]
33. Kerschbaum, F.; Lebzelter, T.; Mekul, L. Bolometric corrections for cool giants based on near-infrared photometry. *Astron. Astrophys.* **2010**, *524*, A87. [[CrossRef](#)]
34. Abia, C.; de Laverny, P.; Romero-Gómez, M.; Figueras, F. Characterisation of Galactic carbon stars and related stars from Gaia EDR3. *Astron. Astrophys.* **2022**, *664*, A45. [[CrossRef](#)]
35. Cantat-Gaudin, T.; Anders, F.; Castro-Ginard, A.; Jordi, C.; Romero-Gómez, M.; Soubiran, C.; Casamiquela, L.; Tarricq, Y.; Moitinho, A.; Vallenari, A.; et al. Painting a portrait of the Galactic disc with its stellar clusters. *Astron. Astrophys.* **2020**, *640*, A1. [[CrossRef](#)]
36. Dias, W.S.; Monteiro, H.; Moitinho, A.; Lépine, J.R.D.; Carraro, G.; Paunzen, E.; Alessi, B.; Vilella, L. Updated parameters of 1743 open clusters based on Gaia DR2. *Mon. Not. R. Astron. Soc.* **2021**, *504*, 256–371. [[CrossRef](#)]
37. Blanco, V.M.; McCarthy, M.F.; Blanco, B.M. Carbon and late M-type stars in the Magellanic Clouds. *Astrophys. J.* **1980**, *242*, 938–964. [[CrossRef](#)]



38. Cristallo, S.; Piersanti, L.; Straniero, O.; Gallino, R.; Domínguez, I.; Abia, C.; Di Rico, G.; Quintini, M.; Bisterzo, S. Evolution, Nucleosynthesis, and Yields of Low-mass Asymptotic Giant Branch Stars at Different Metallicities. II. The FRUITY Database. *Astrophys. J. Suppl. Ser.* **2011**, *197*, 17. [[CrossRef](#)]
39. Hunt, E.L.; Sabine, R. Improving the open cluster census. II. An all-sky cluster catalogue with Gaia DR3. *Astron. Astrophys.* **2023**, *673*, A114. [[CrossRef](#)]

**Disclaimer/Publisher's Note:** The statements, opinions and data contained in all publications are solely those of the individual author(s) and contributor(s) and not of MDPI and/or the editor(s). MDPI and/or the editor(s) disclaim responsibility for any injury to people or property resulting from any ideas, methods, instructions or products referred to in the content.